

Improved anode performance of Ni–P-coated Si thick-film electrodes for Li-ion battery

Hiroyuki USUI, Naoki UCHIDA, and Hiroki SAKAGUCHI*

Department of Chemistry and Biotechnology, Graduate School of Engineering, Tottori University
4-101 Minami, Koyama-cho, Tottori 680-8552, Japan

*Corresponding author. Tel./Fax: +81-857-31-5265; e-mail: sakaguch@chem.tottori-u.ac.jp

Abstract

To improve the deviation of cycling performances as Li-ion battery anode, we controlled the morphology of Ni–P layers deposited on Si particles in thick-film electrodes prepared by a gas-deposition method. The spotty Ni–P layers were uniformly coated on Si particles by an electroless deposition in a neutral bath. The resulting electrodes using Ni–P-coated Si exhibited excellent cycling performances and their good reproducibility. The reason for the improvement of performances is probably that the Ni–P layers can effectively release a stress generated by alloying/dealloying reactions of Li with Si.

Keywords: Si anode; Electroless deposition; Gas-deposition; Li-ion battery

1. Introduction

Silicon has a notable potential as an anode of Li-ion battery due to its huge theoretical capacity.^{1,2} It is, however, difficult to apply Si for practical anodes because Si has some critical disadvantages: a low electronic conductivity, a low diffusion coefficient of Li, and drastic changes in its specific volume during Li-insertion/extraction. The volumetric changes cause a high stress, a severe pulverization, and an electrical isolation in Si anode, thereby resulting in a poor charge–discharge performance. To overcome these problems, some researchers have recently studied carbon conductive additives^{3–5} and functional binders⁶ for Si-based anodes. As other approach, we have prepared composite thick-film electrodes of Si coated with Ru,⁷ Cu,⁸ Ni⁹ layers, and Ni/Cu multilayer¹⁰ by using an electroless deposition (ELD) method and a successive gas-deposition (GD) method.¹¹ It has been revealed that the coated metal layers on the Si particles can play important roles in increasing the electrical conductivity of active material⁸ and in releasing the stress induced by the volumetric changes of Si.⁹ Among some coated layers, we have obtained the best performance when Ni–P with the amount of 0.2 wt.% was coated on Si particles by ELD in an acid bath. There is, however, a large deviation of its anode performance because of the small amount and a segregated morphology of the coated layer. Nevertheless, the small amount of coated layer is preferable for application. Consequently, it is required to improve the performance without increasing the coating amount. In this study, we changed the ELD condition from the acid bath to a neutral bath for Ni–P coating on Si particles, and attempted to improve the deviation of the performance by changing the morphology of coated layer.

2. Experimental

The ELD of Ni–P on Si particles was performed by adding a reducing agent of BH_4^- solution into a solution containing Si particles, Ni^{2+} ions, and H_2PO_2^- ions. The detailed conditions have been described in previous papers.⁹ In case of the conventional acid bath, we used H_2SO_4 aqueous

solution so that the pH value set to be 1.4. On the other hand, we newly carried out ELD in a neutral bath without H₂SO₄, and the pH value was 6.6. The elemental analysis of the coated particles was made by an inductively coupled plasma atomic emission spectroscopy (ICP-AES, Spectro Ciros CCD, Rigaku Ltd.). For both samples prepared in acid and neutral baths, we detected 99.8 wt.% Si, 0.18 wt.% Ni, and 0.02 wt.% P by the ICP-AES analysis. We can thus discuss the morphology of the coated layers because no change in the coated amount was found. The morphology and crystal structure of the coated layers were observed by a transmission electron microscopy (TEM, JEOL-2010, JEOL Ltd.). Thick-film electrodes of Ni–P-coated Si were prepared on Cu foil substrates by the GD method.¹¹ The weight of the deposited active materials in this study was 0.017–0.020 mg. The indentation elastic modulus of the electrodes before charge–discharge cycle was measured by an indentation test using a dynamic ultra-micro hardness tester (DUH-211S, Shimadzu Co. Ltd.).⁹

Electrochemical measurements were carried out with a beaker-type three-electrode cell. The working electrodes were the obtained thick-film electrodes. Both counter and reference electrodes were 1-mm-thick Li metal sheets (Rare Metallic, 99.90%). We used LiClO₄ dissolved in propylene carbonate (PC; C₄H₆O₃, Kishida Chemical Co., Ltd.) at concentration of 1 mol dm⁻³ as the electrolyte. Constant current charge–discharge tests were performed using an electrochemical measurement system (HJ-1001 SM8A, Hokuto Denko Co., Ltd.) under a constant current of 1.6 A g⁻¹ at 303 K with the cutoff potentials set as 0.005 V vs. Li/Li⁺ for charge and 3.400 V vs. Li/Li⁺ for discharge.

3. Results and Discussion

Figures 1(a) and 1(c) show TEM images of Ni–P-coated Si (Ni–P/Si) particles prepared by ELD in neutral and acid baths, respectively. In case of the acid bath, Ni–P was obviously segregated on Si particles. In a sense, the segregated morphology of Ni–P is a favorable because Si particles have

larger area of denuded surface where Li ions can insert and extract. However, the Ni–P layer seems to be too segregated in this case. A hydrolysis reaction of BH_4^- also generally occurs in acid baths, which is associated with inhomogeneous oxidation of BH_4^- and H_2 gas generation.^{12,13} By these phenomena on Si particles in this study, Ni–P layers were not uniformly deposited on the surface particles to form segregated layers. We expect that the significant segregation of Ni–P causes the large deviation of the anode performance of the electrode in case of the acid bath. In contrast, spotty Ni–P particles with a smaller size will be more uniformly deposited on Si particles in case of the neutral bath. Figures 1(b) and 1(d) give corresponding selected area electron diffraction (SAED) patterns of the Ni–P-coated particles obtained in the neutral and acid baths shown in Fig. 1(a) and 1(c), respectively. The *d*-spacings derived from the diffraction spots are summarized in Table 1. In both cases, Ni (Inorganic Crystal Structure Database, ICSD No. 00-004-0850) and Ni_3P (No. 01-074-3245) phases were detected for the coated layer. This revealed that the coated layers consisted of mixture of Ni and Ni_3P .

Figure 2 shows charge–discharge curves at the first cycles for the thick-film electrodes of Ni–P-coated Si particles. For comparison, the curve was also plotted for the result of a pristine Si electrode. In every case, potential plateaus appeared at 0.1 and 0.4 V vs. Li/Li^+ in charge (lithiation) and discharge (delithiation) processes. It has been recently reported that lithiation plateaus at 0.1 V originate from the phase transition from crystalline Si to $\text{Li}_{15}\text{Si}_4$ ($\text{Li}_{3.75}\text{Si}$)^{14,15} and/or amorphous Li-Si ^{15,16} at room temperature, and that delithiation plateaus at 0.4 V are attributed to Li-extraction from these phases. The crystallization of the equilibrium intermetallic phases is kinetically forbidden.^{15,16} Smaller charge/discharge capacities in case of acid bath are possibly caused by the segregated Ni–P with the larger size: Li-insertion/extraction reactions are disturbed by Li-inactive Ni in the segregated Ni–P layers on Si particles.

Figure 3 gives cycling performances of the Ni–P/Si electrodes. To evaluate the reproducibility in each case, cycling performances were measured for another equivalent electrode as 2nd run

sample. When Ni–P layers were locally deposited on Si particles in the acid bath, we have observed a large deviation of the discharge capacities between 1st and 2nd runs: the differences at the first cycle and 1000th cycle were about 600 and 300 mA h g⁻¹, respectively. In contrast, the excellent reproducibility of anode performance was obtained for the electrode prepared by using neutral bath in which the spotty Ni–P layers uniformly deposited. The differences were approximately 300 and 100 mA h g⁻¹ at the first cycle and 1000th cycle. We succeeded in obtaining reproducibly the excellent performances by the uniform deposition of the spotty Ni–P layers on Si particles. In particular, it is noteworthy that the 1st run electrode maintained a capacity of 780 mA h g⁻¹ even at 1000th cycle, and that the electrode exhibits the best performance in various electrodes which the authors have ever examined.

The improved performances appear to be caused by an increasing mechanical durability of thick-film electrodes because pulverization of Si is one of the main reasons for degrading performance in Si-based anodes. We measured the indentation elastic modulus of the Ni–P/Si thick-film electrodes. A higher indentation elastic modulus of 37 ± 13 kN mm⁻² was obtained for the electrode of Ni–P/Si prepared in the acid bath compared with the pristine Si electrode (8 ± 0.6 kN mm⁻²). On the other hand, its standard deviation was relatively large. The indentation loading/unloading measurements were carried out in this study for various points on electrode surface. It is suggested that Ni–P layers are sandwiched between Si particles in thick-film electrodes. Thus, varied elastic modulus was measured from the electrode containing segregated Ni–P layers. This indicates that the segregated layers have an unstable function to release the stress induced by the volumetric change of Si. We consider that the varied elastic modulus is a main reason for the deviation of the cycling performances. In case of the neutral bath, the Ni–P/Si electrode exhibited a value of 46 ± 3 kN mm⁻², a high elastic modulus and smaller standard deviation. The spotty Ni–P layers are uniformly distributed between Si particles in the electrodes. This means that the layers

make the Si particles stick to each other, and that the layers can effectively release the stress from Si in whole region of the thick-films. We conclude therefore that excellent cycling performances were reproducibly attained for the electrodes consisted of Si coated with spotty Ni–P layers prepared in the neutral bath. In general, Si-based anodes show varied electrode performance owing to its disadvantages, the low conductivity, the low diffusion coefficient of Li, and the drastic volume changes during Li-insertion/extraction. It is noteworthy that we have simultaneously achieved both the excellent cycling performances and the good reproducibility by the morphological control of Ni–P layers.

Conclusion

The spotty Ni–P layers were confirmed to deposit on Si particles in the neutral bath. Excellent cycling performances and their good reproducibility were achieved in the thick-film electrodes consisted of the Ni–P/Si particles. The improved performances are attributed to effectively-released stress from Si by the Ni–P layers.

Acknowledgments

This work was supported in part by the Li-EAD program of the New Energy and Industrial Technology Development Organization (NEDO) of Japan. This work has been partially supported by a Grant-in-Aid for Scientific Research from the Ministry of Education, Culture, Sports, Science and Technology (MEXT) of Japan. The authors also gratefully acknowledge Prof. K. Ichino for his kind assistance with TEM observations.

References

- 1 T. Takamura, S. Ohara, M. Uehara, J. Suzuki, and K. Sekine, *J. Power Sources*, **129**, 96 (2004).

- 2 D. Larcher, S. Beattie, M. Morcrette, K. Edström, J.-C. Jumas, and J.-M. Tarascon, *J. Mater. Chem.*, **17**, 3759 (2007).
- 3 T. Inose, D. Watanabe, H. Morimoto, and S. Tobishima, *J. Power Sources*, **162**, 1297 (2006).
- 4 Q. Si, K. Hanai, T. Ichikawa, A. Hirano, N. Imanishi, Y. Takeda, and O. Yamamoto, *J. Power Sources*, **195**, 1720 (2010).
- 5 M. Saito, K. Nakai, T. Yamada, T. Takenaka, M. Hirota, A. Kamei, A. Tasaka, and M. Inaba, *J. Power Sources*, **196**, 6637 (2011).
- 6 S. Komaba, N. Yabuuchi, T. Ozeki, Z.-J. Han, K. Shimomura, H. Yui, Y. Katayama, and T. Miura, *J. Phys. Chem. C*, **116**, 1380 (2012).
- 7 H. Usui, Y. Kashiwa, T. Iida, and H. Sakaguchi, *J. Power Sources*, **195**, 3649 (2010).
- 8 H. Usui, H. Nishinami, T. Iida, and H. Sakaguchi, *Electrochemistry*, **78**, 329 (2010).
- 9 H. Usui, M. Shibata, K. Nakai, and H. Sakaguchi, *J. Power Sources*, **196**, 2143 (2011).
- 10 H. Usui, N. Uchida, and H. Sakaguchi, *J. Power Sources*, **196**, 10244 (2011).
- 11 H. Sakaguchi, T. Toda, Y. Nagao, and T. Esaka, *Electrochem. Solid-State Lett.*, **10**, J146 (2007).
- 12 J. E. A. M. van den Meerakker, *J. Appl. Electrochem.*, **11**, 395 (1981).
- 13 K. S. Freitas, B. M. Concha, E. A. Ticianelli, and M. Chatenet, *Catalysis Today*, **170**, 110 (2011).
- 14 Y.-M. Kang, S.-M. Lee, S.-J. Kim, G.-J. Jeong, M.-S. Sung, W.-U. Choi, and S.-S. Kim, *Electrochem. Commun.*, **9**, 959 (2007).
- 15 V. L. Chevrier, J. W. Zwanziger, and J. R. Dahn, *J. Alloys Compd.*, **496**, 25 (2010).
- 16 M. K. Datt and P. N. Kumta, *J. Power Sources*, **194**, 1043 (2009).

Figure caption

Table 1. Summary of *d*-spacings (nm) and crystal phase derived from analysis of selected area electron diffraction for Ni–P/Si particles. The table also describes ICSD standard *d*-spacings in Ni (00-004-0850), Ni₃P (01-074-3245), and Si (00-027-1402).

Figure 1. TEM images of Ni–P/Si particles prepared by ELD in (a) neutral and (c) acid baths. The pH values of neutral and acid baths are 6.6 and 1.4. (b),(d) Corresponding SAED patterns of the particles shown in (a) and (c).

Figure 2. Charge–discharge curves at the first cycles of thick-film electrodes consisted of Ni–P/Si particles prepared in neutral and acid ELD baths.

Figure 3. Cycling performances of Ni–P/Si thick-film electrodes. To evaluate reproducibility, cycling performances were measured for another equivalent electrode as 2nd run sample.

Table 1. Summary of *d*-spacings (nm) and crystal phase derived from analysis of selected area electron diffraction for Ni–P/Si particles. The table also describes ICSD standard *d*-spacings in Ni (00-004-0850), Ni₃P (01-074-3245), and Si (00-027-1402).

Ni–P/Si (neutral)	Ni–P/Si (acid)	ICSD standard	
<i>d</i> -spacing / nm	<i>d</i> -spacing / nm	<i>d</i> -spacing / nm	crystal phase (<i>h k l</i>)
0.3070	0.3070	0.3135	Si (1 1 1)
0.1740	0.1797	0.1733	Ni ₃ P (3 1 2)
0.1580	0.1563	0.1638	Si (3 1 1)
0.1260	---	0.1246	Si (3 3 1)
0.1106	0.1160	0.1096	Ni ₃ P (0 0 4)
0.1042	0.1042	0.1062	Ni (3 1 1)
0.0946	0.0972	0.0960	Si (4 4 0)
0.0898	0.0860	0.0881	Ni (4 0 0)
0.0836	---	0.0808	Ni (3 3 1)

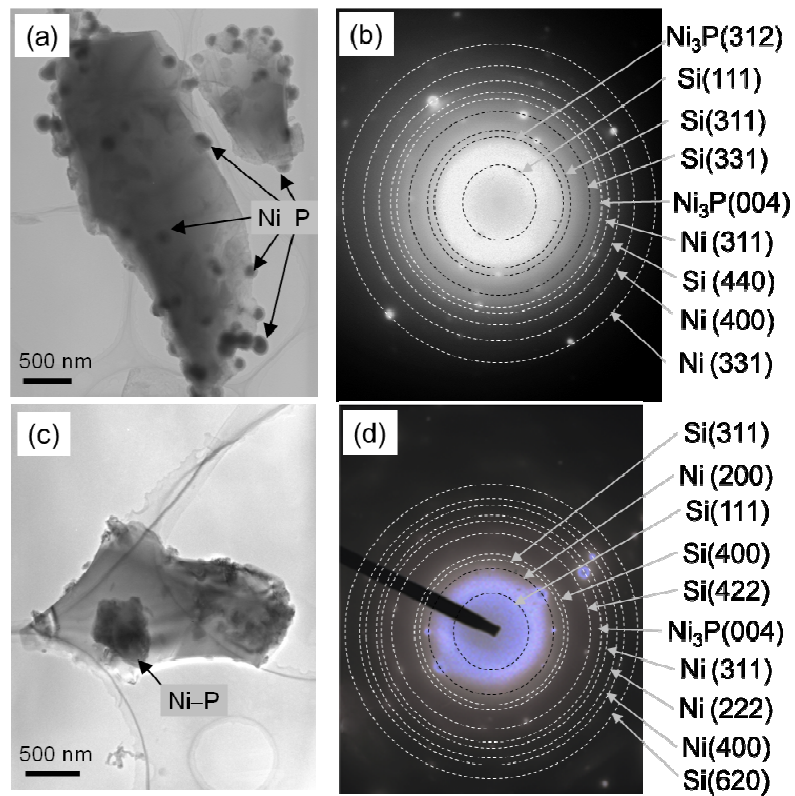


Figure 1. TEM images of Ni–P/Si particles prepared by ELD in (a) neutral and (c) acid baths. The pH values of neutral and acid baths are 6.6 and 1.4. (b),(d) Corresponding SAED patterns of the particles shown in (a) and (c).

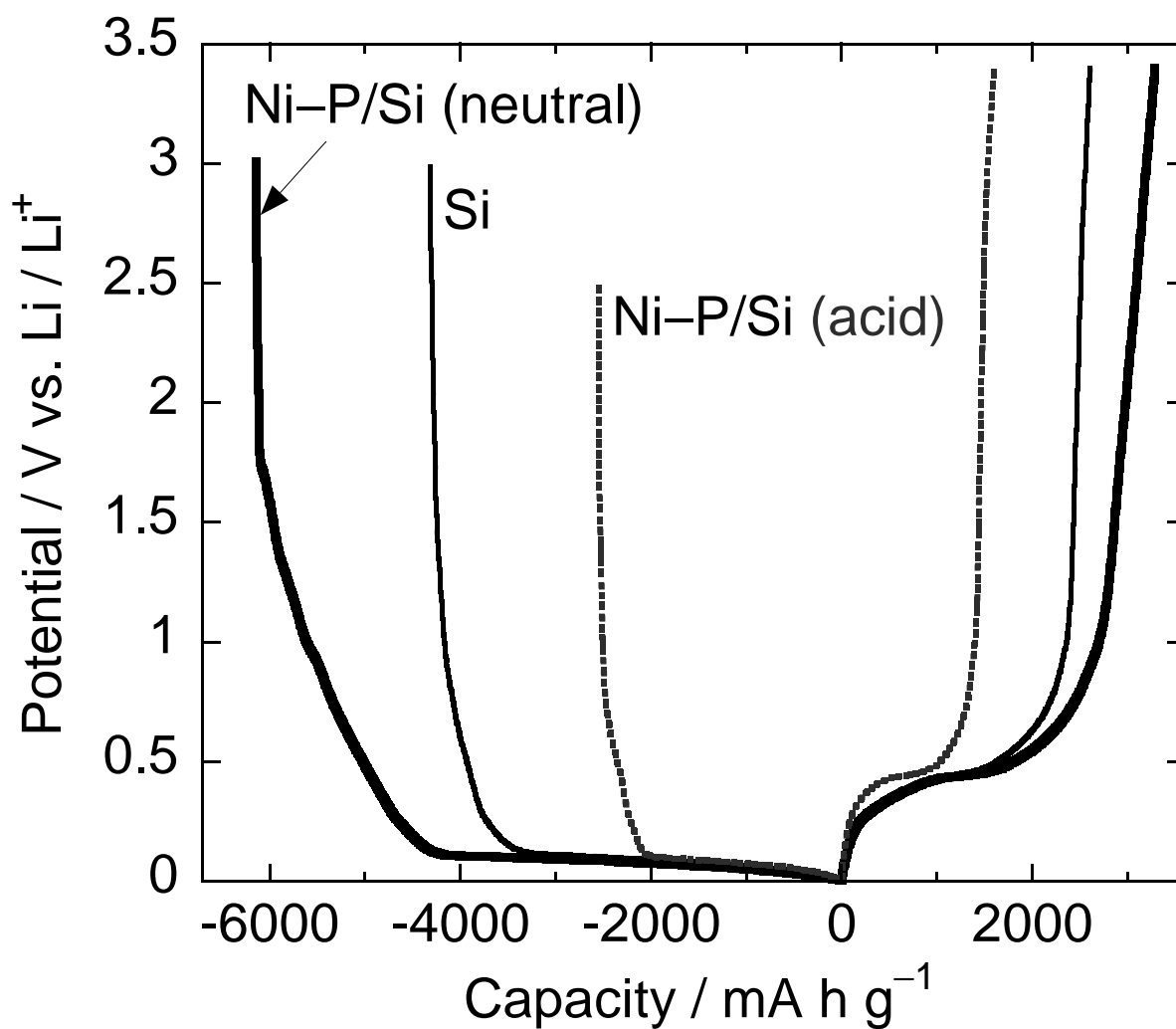


Figure 2. Charge–discharge curves at the first cycles of thick-film electrodes consisted of Ni–P/Si particles prepared in neutral and acid ELD baths.

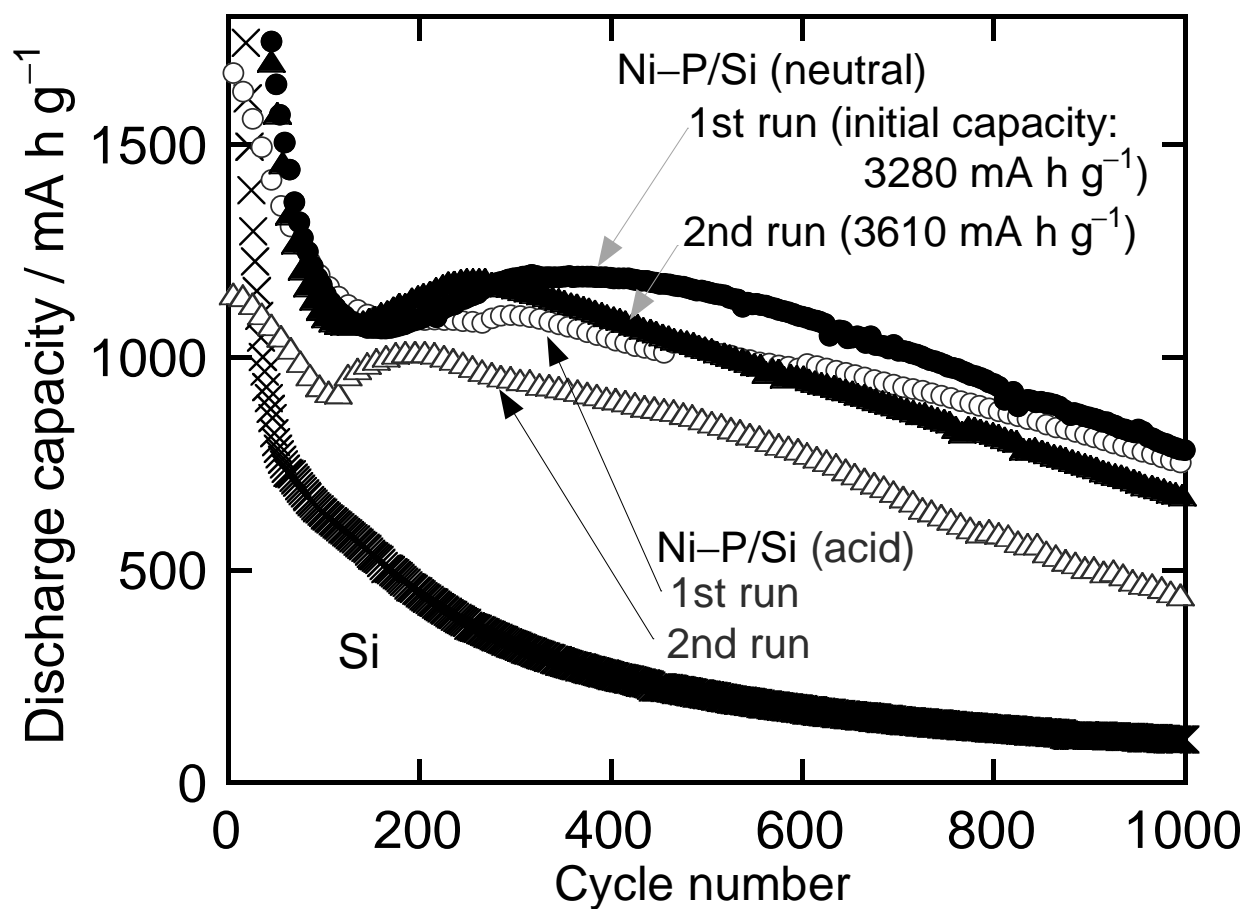


Figure 3. Cycling performances of Ni-P/Si thick-film electrodes. To evaluate reproducibility, cycling performances were measured for another equivalent electrode as 2nd run sample.